ISSN 1590-8844
International Journal of Mechanics and Control, Vol. 24, No. 02, 2023

https://doi.org/10.69076/jomac.2024.0019

DESIGN AND EXPERIMENTAL VALIDATION OF A FIBER OPTIC PRESSURE SENSOR WITH FBG TECHNOLOGY

M. Bertone* A. Aimasso* A. Rovera** C.G. Ferro* M.D.L. Dalla Vedova*

* Department of Mechanical and Aerospace Engineering, Politecnico di Torino

** Department of Material and Science Technology, Politecnico di Torino

ABSTRACT

The development of smart systems through the use of components capable of autonomously generating data regarding their own performance is an extremely innovative aspect in the development of complex machines and their related control algorithms. This goal can be achieved by widely employing integrated and minimally invasive sensing technology that can be seamlessly integrated into control logic. In this regard, the use of monomodal optical fiber and Fiber Bragg Grating (FBG) sensors is the best technical solution currently available. This paper describes the development of a pressure sensor created by using an FBG sensor embedded in a silicone resin base. When subjected to pressure, the deformability of the resin induces a strain in the FBG sensor. The aim is therefore to verify the presence of a correlation between the applied pressure and the optical data generated by the grating. The sensor was fabricated by casting resin into a mold created through additive manufacturing, and then placed in an additional casing, also fabricated through additive manufacturing. The product underwent a specific experimental testing campaign, with the data analyzed statistically. The results highlighted excellent sensitivity, validating the proof of concept and providing an estimation of the sensor's current performance.

Keywords: FBG, Optical sensor, Aerospace Engineering, System Engineering

1 INTRODUCTION

The real-time measurement of physical parameters describing the performance of a mechanical system is crucial for the development of control logics and, more broadly, for system engineering activities [1-2]. In particular, innovative control logics can be developed through the creation of "smart" components, capable of autonomously generating a large amount of data. These data, through appropriate analysis algorithms or, possibly, using AI, can provide complex information about the macroscopic behavior of the system and generate diagnostic and prognostic algorithms to increase the level of safety and reliability of the final product. A smart component is capable of providing precise and distributed measurements at a large number of points related to specific physical parameters.

Contact authors: Matteo Bertone[1], Alessandro Aimasso[1]

[1]Department of Mechanical and Aerospace Engineering, Politecnico di Torino.

E-mail: matteo.bertone@polito.it, alessandro.aimasso@polito.it

To achieve this goal, it is necessary to have an extremely versatile instrumentation methodology, minimally invasive, adaptable to different geometries, and capable of measuring very different physical parameters [3]. Fiber optic sensing can satisfy this requirement thanks to the specific characteristics of this material. Additionally, in certain situations, fiber optic integration can occur directly during the production process of the component itself. Indeed, the low invasiveness of the fiber cable, combined with the possibility of having many sensors on the same communication line, allows for numerous measurement points on a single component with negligible invasiveness [4-5]. Considering the extreme versatility of the product and the short response time of FBG sensing, it becomes crucial to integrate such sensors into the control loop [6]. To achieve this, however, it is necessary not only to integrate them into the component itself but also to develop specific packaging that allows the development of an optical sensor for a specific parameter. In the last two decades, the use of optical fiber has significantly increased, finding applications in various technological sectors, starting from communications and the internet. Indeed, an increasing number of engineering solutions - in sectors not only industrial -now rely on the use of optical technology, with applications ranging from medicine to lighting technology, up to structural monitoring of civil infrastructures [7-12].

More recently, even the aerospace sector has begun to look with interest at the implementation of optical technology in its subsystems [13-16]. Optical fiber, in fact, presents significant advantages for monitoring different physical parameters within system engineering activities [17]. In particular, the optical fiber extreme lightness, versatility, and minimal invasiveness allow its application in systems that are radically different from each other, in mechanical, aeronautical or space sectors. Furthermore, given its purely optical nature, it does not present electromagnetic compatibility problems, allowing to be installed near electrical and electronic components without risking to undergo or to generate interference. Moreover, the glassy composition of optical fiber also ensures the possibility of operating at extremely high temperatures (several hundred degrees) and the impossibility of generating sparks and therefore to possible fires. This last characteristic is therefore extremely important for monitoring tanks and measuring fuel levels inside them. The combination of these characteristics, together with the high sensitivity to parameters such as temperature, strain, vibrations, etc., makes optical sensing particularly suitable for ensuring high performance even when employed in a hostile environment: a requirement typical of the aerospace sector [18-19]. The main purpose of this work is the development, realization and verification of a pressure sensor developed by integrating a Fiber Bragg Grating sensor in a polymeric substrate. In particular, the specific idea is to integrate the ensemble of polymeric resin and FBG sensor in a customable mold. In this way, when the system is subjected to a pressure variation, the deformation of the resin is applied to the FBG, so generating an output that can be correlated to the pressure variation itself. Consequently, the work could be defined as a proof of concept aimed at the ability to develop a pressure sensor using fiber optic for both a gas pressure sensor and a liquid-induced pressure sensor, and thus as a level sensor (e.g., fuel). The overall work was organized as follow:

- Definition of sensibility strategy and high level sensor geometry;
- Realization of CAD;
- Physical prototype realization;
- Test campaign;
- Overall performance evaluation.

2 OPTICAL FIBER AND SENSORS FOR SYSTEMS

The optical fiber is a cylindrical waveguide composed of several concentric layers, which allows the transmission of a light signal through a mechanism of multiple reflections in the innermost layer. In this work, a single-mode optical fiber with the following characteristics was employed:

- Inner core with a diameter of 9 μm, enabling the transmission of a single-mode signal
- Cladding with a diameter of 125 μm
- Coating with an additional diameter of 125 μm made of polyacrylate

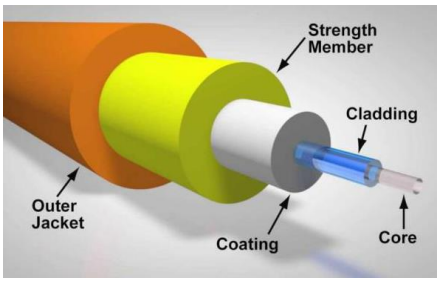

Figure 1 Structure of optical fiber.

The *core* represents the innermost part of the fiber and it is within this core that the light physically propagates. Generally, it is composed of a glassy or polymeric material. The *cladding* is the intermediate layer, and its presence is essential to ensure that the light beam remains confined within the core. Finally, the *coating* represents the outermost layer: it does not contribute in any way to the transmission of the light signal, but its presence is crucial to counteract the extreme fragility of the fiber. Additionally, due to the very low bending resistance of the fiber, besides the coating, an additional layer of outer sheathing may sometimes be necessary.

The sensors used in this study are created directly within the optical fiber. An FBG sensor, or *Fiber Bragg Grating*, is essentially a periodic modulation of the refractive index of short trait (5 mm) in the inner core [20-21]. This modulation acts as a frequency-selective filter: when the light passes through it, all frequencies of the electromagnetic spectrum can pass through, except for a specific one that is reflected back towards the source. This reflected frequency constitutes the physical output of the sensor. In this way, bands of material with an alternating refractive index are created at regular intervals, typically ranging from 0.5 μm to a few μm. The collection of these bands of material with different refractive indices constitutes the FBG sensor. and is quantified in terms of wavelength according to the equation:

$$\lambda_B = 2n_{eff}\Lambda \tag{1}$$

As can be clearly seen, the Bragg frequency is directly proportional to the grating pitch. Any external factor that modifies this length results in a change in the frequency reflected by the grating. For this reason, FBG sensors are primarily used to monitor temperature variation and mechanical deformation, the two main physical parameters that affect the variation in grating pitch.

Mathematically, the variation in the wavelength reflected by the sensor is quantified as:

$$\Delta\lambda/\lambda_b = K_T\,\Delta T + K_\varepsilon\,\Delta\varepsilon \tag{2}$$

where $\Delta\lambda/\lambda$ is the parameter measured by the instrumentation. When an FBG sensor is applied to the piece being monitored, the value of $\Delta\lambda/\lambda$ depends on the combination of two contributions: the temperature variation ΔT and the mechanical deformation $\Delta\varepsilon$.

The ability of gratings to be sensitive to different physical parameters using the same operating principle is evident. Therefore, it is essential to define effective calibration under conditions of sensitivity to only one of these parameters, and then develop a proper technique for compensation and decoupling of effects. At Politecnico di Torino, authors started in several works to use FBGs. In particular, great effort was firstly addressed to define the aforementioned calibration and effects decoupling technique [22-28]. Then, the research group started to define a more complex strategy, in order to use optical sensors as input data of “smart logics” to monitor overall systems performances [29-30].

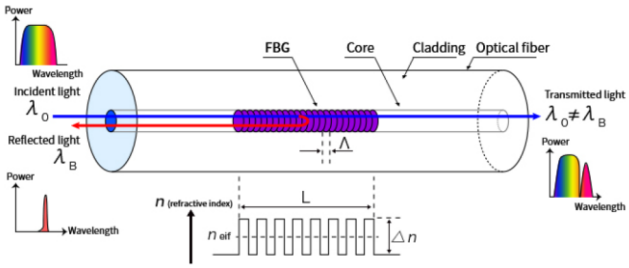

Figure 2 Working principle of FBG.

3 PRESSURE SENSOR REALISATION

To ensure the greatest possible compatibility with various operating conditions, particular attention has been paid to chemical inertness. Another aspect that had to be taken into account was the ease of realizing complex geometries. The main characteristics sought in the material were therefore its moldability and the ability to degas without the need for dedicated equipment. The material selected for the sensor construction was a two-component silicone resin called "MasterSil 151". The use of a silicone material allows for reasonable chemical inertness, enabling operation even in the presence of oils and organic solvents. At the same time, the specific resin selected does not introduce any limitations on the achievable geometries due to its low viscosity during the polymerization phase and the reasonable working time before achieving a significant degree of polymerization. The main factors that guided the definition of the sensor's geometry were as follows:

- Ease of assembly
- Adaptability to different membrane geometries
- Compactness
- Possibility of serial insertion with other sensors
- Fiber protection from damage

The sensor consists of three main elements: a base, the membrane containing the sensor and a closure and fixing element. The *base* portion contains the controlled atmosphere chamber which is subsequently sealed by the membrane itself. The choice of *membrane* geometry was made to maximize sensitivity while providing reasonable protection to the FBG.

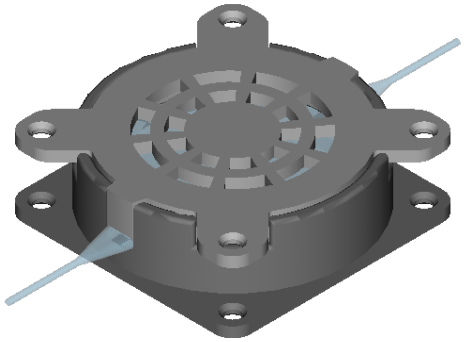

Figure 3 Final sensor assembly.

For this purpose, a cylindrical geometry with a diameter of 60mm was chosen. To ensure accurate sensor positioning, two guides for the optical fiber were provided. These guides, in addition to ensuring positioning repeatability, also protect the fiber as it exits the membrane, limiting possible sources of shear stress. The plastic nature of the finished product finally allows for the separation between different environments, the reference and the measuring one. The sensor is completed by a *closure* and fixing element. The closure element features a lattice structure designed to dampen any dynamic contributions from the measurement environment, while simultaneously protecting the membrane from potential mechanical damage.

For the prototype construction, the use of 3D printing processes, specifically stereolithographic printing (SLA) with resin, was chosen. The use of SLA allows for the production of prototypes with a high level of dimensional accuracy necessary to ensure the sealing of the different elements. The construction of the actual membrane, the only element not obtained directly from SLA, required the design and production of a dedicated mold. It consists of two portions that join along the membrane's midline, where the negative of the membrane is formed. In the upper portion, various channels necessary for the silicone casting process were created. Firstly, a "reservoir" was provided to contain a reserve of silicone to compensate for resin shrinkage during the curing phase. Secondly, ventilation channels were created to facilitate the escape of air trapped in the resin during the mixing process, as well as to allow for the complete emptying of any air pockets.

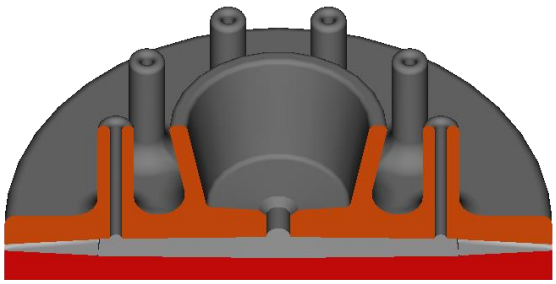

Figure 4 Mould for resin.

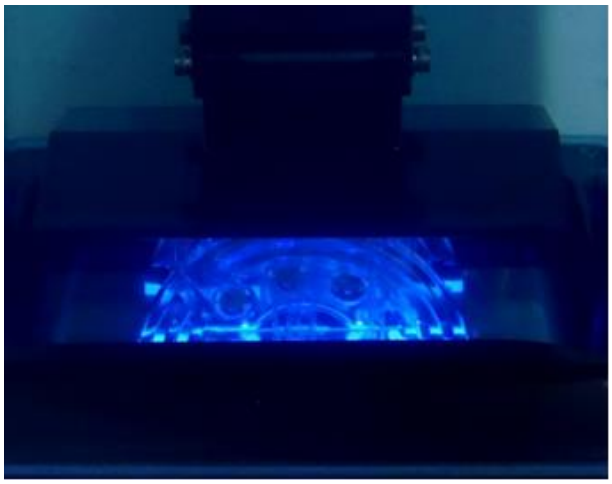

Figure 5 Additive manufacturing process.

4 TEST CAMPAIGN

The data acquisition process was meticulously prepared by developing an experimental set up and the relative test campaign. The experimental set up was though in order to be able to guarantee the interaction between the optical data acquisition system, the sensor and the pneumatic system. The optical data acquisition system was mainly constituted by the Smart Scan laser interrogator. This advanced instrument played a pivotal role in capturing and analyzing the outputs generated by the FBG sensors with precision and accuracy. Each optical fiber line was connected to one of the designated "outputs" or channels of the interrogator through FC/APC connectors, ensuring seamless and uninterrupted data transmission. Through its channels, the interrogator sent a light source inside the fibers. Contextually, it can detect the reflected wavelengths coming from each FBG, allowing to quantify their outputs and to create data to be analyzed. The results are sent to the user PC thanks a LAN connection, ensuring real-time access to sensor data. The sensor was placed in a pressurized and hermetic tank, with a feedthrough employed to let the fiber to arrive to the interrogator. Moreover, a tube linked to the laboratory's pneumatic system was introduced inside the tank for pressure regulation. The pneumatic system available at Politecnico di Torino allow a pressure variation from 0 to 9 bar. However, to validate the developed sensor, lower pressure sere required. In this regard, a fine regulation valve, linked to a manometer, were added between the main pneumatic system and the connection to the tank. Figure 6 summarize the overall architecture of the experimental setup. The test campaign was designed with the aim of repeatedly stressing the sensor at defined pressure values with both charging and discharging cycles. The applied pressure was varied from 0 to 200 mbar, with intermediate steps every 50 mbar (Table I). Each step was maintained for 90 seconds, with the aim of stabilizing both the pneumatic system and the optical data read by the interrogator.

Furthermore, data acquisition from the interrogator was set at 2.5 Hz, a very low value for the instrument but still sufficient to be able to acquire sufficient data to be able to conduct appropriate statistical analyses. The experimental data obtained were therefore first acquired using a specific MATLAB code. Through it, the optical values measured during each step were identified and saved. Subsequently the final results were calculated through the use of the MINITAB software, in order to obtain:

- The boxplots of each pressure step;
- The data statistical distribution of each pressure step;
- The sensor calibration curve.

The post processing methodology, together with the discussion of the results, are reported in detail in the following chapter.

Table I - Cycle test steps

# Step	Pressure [mbar]	Duration [s]
1	0	90
2	50	90
3	100	90
4	150	90
5	200	90
6	150	90
7	100	90
8	50	90
9	0	90

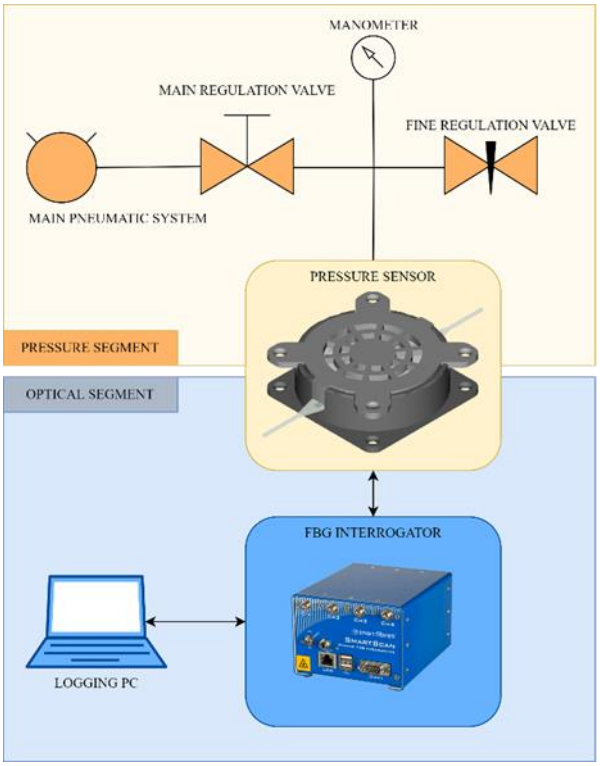

Figure 6 Experimental set up.

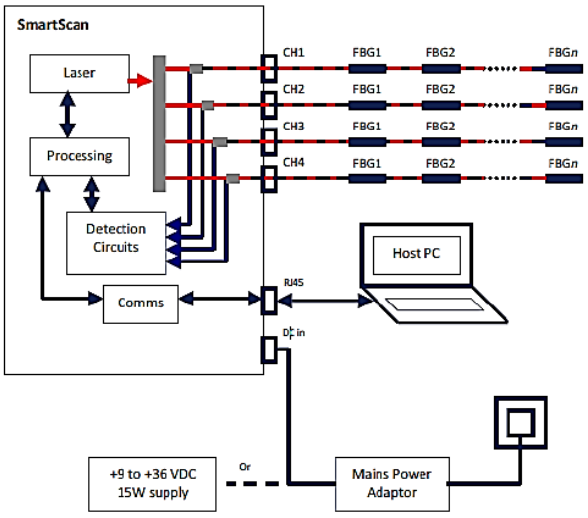

Figure 7 Optical data acquisition system.

5 RESULTS AND DISCUSSION

The experimental raw data consists in the reflected wavelength values generated by the FBG sensor over the entire experimental test (Fig. 7). The performance of the sensor was firstly analyzed by considering this simple optical response of the sensor. Then, the distribution of the data relating to each step was carefully analyzed to validate the statistical distribution. Finally, great attention was done to assess the repeatability of the measurements. Thanks to data collected, the sensor calibration curve was constructed on the basis of the boxplots results of each stable step. Using this interpolation, the previous optical values were converted into pressure values: the statistical analysis was therefore repeated on these reconverted values. Moving to discuss about experimental data, graph in Figure 8 shows a significant sensitivity of the sensor response to each step of applied pressure, as well as a good reversibility of the measures. By observing the raw experimental data, it is possible to observe the wavelength's variation during the test campaign.

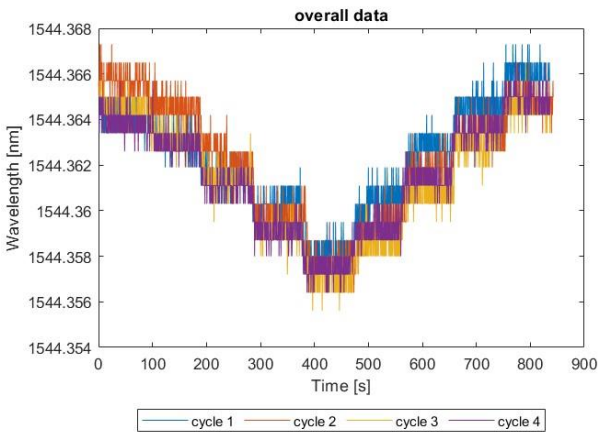

Figure 8 Raw data.

In particular, it is clearly understandable the wavelength variation in consequence of the pressure applied by the system on the sensor. Even in a qualitative way, the FBG proved its sensitivity to pressure variations of about 50 mmbar. Based on this initial positive preliminary result, the following steps were performed:

- Selection of data from stability intervals.
- Creation of statistical boxplots for each of the pressure steps.
- Statistical analysis of sampled data in each step.

The stability stages were chosen by taking into account the central 40 seconds of acquisition for each step, yielding a total of 100 points examined for each pressure step considered. Thus, each boxplot is constructed using 400 experimental data, taking into account the four-cycle overlap. The numerical results are reported in table II and graphed in Figure 9.

Numerous and significant considerations can be derived from results just presented. Firstly, the breadth of the experimental data distribution confirms the system's sensitivity to the progressive variation in pressure of 50 millibars applied to the sensor. Moreover, the same distribution also allows defining this pressure threshold as the sensitivity of the developed measuring instrument, so validating the initial qualitative result.

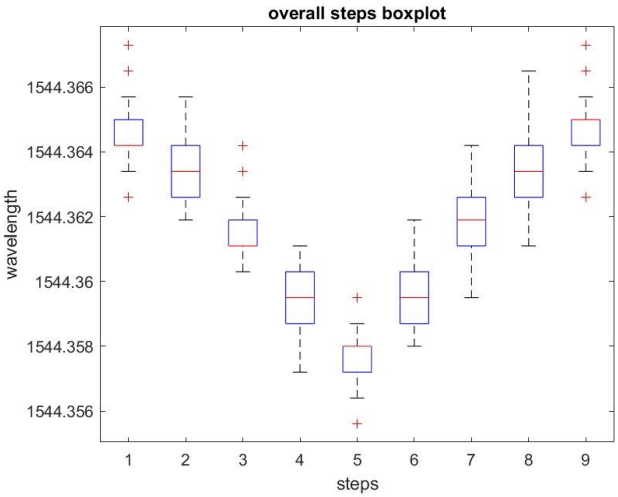

Figure 9 Boxplot of experimental data.

Table II – Data of boxplot

Variable	Total count	SE mean	St Dev	Variance	Range
P1	400	4.3e-5	8.68e-4	1e-6	4.7e-3
P2	400	4.2e-5	8.41e-4	1e-6	3.8e-3
P3	400	3.4e-5	6.90e-4	1e-6	3.9e-3
P4	400	3.7e-5	7.35e-4	1e-6	3.9e-3
P5	400	3.5e-5	7.07e-4	1e-6	3.9e-3
P6	400	4.2e-5	8.49e-4	1e-6	3.9e3
P7	400	4.5e-5	8.93e-4	1e-6	4.7e-3
P8	400	4.4e-5	8.83e-4	1e-6	5.4e-3
P9	400	5.0e-5	9.94e-4	1e-6	4.7e-3

In fact, the observed range of uncertainty between the 25th and 75th percentiles corresponds to an uncertainty in the value of the measured wavelength comparable to the measurement uncertainty of the interrogator used. The analysis of the data for each step, constructed by overlapping different measurement cycles, both during loading and unloading phases, has revealed the great repeatability of the data generated by the proposed setup. Additionally, the distribution of median values of each boxplot indicates the possibility of identifying an almost linear correlation between the pressure applied by the system and the measured wavelength variation. Finally, occasional outliers occur due to local instabilities in the pneumatic line. Analyzing individual steps, a generally Gaussian distribution of the acquired experimental points over the 4 trials can be observed. In particular, a table with sigma values is obtained.

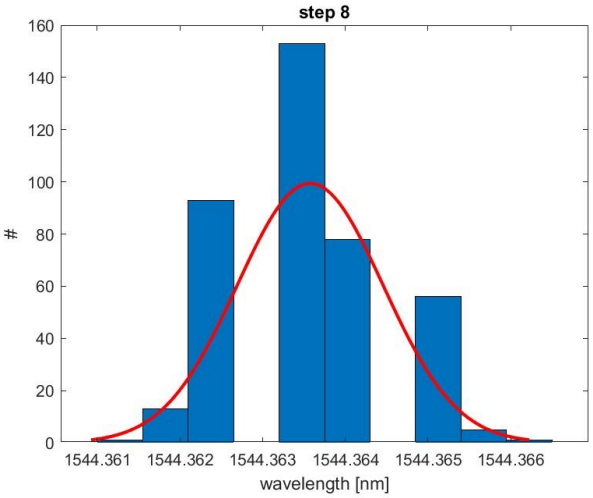

Figure 10 Normal distribution of a single step.

As already highlighted by the values of the boxplots, a nearly linear trend is observed in the analyzed pressure range. Therefore, using the median data of the individual boxplots (referring to stable steps), a sensor calibration curve has been defined. This curve has proven to be linear; consequently, the statistical analyses were repeated using the values converted into pressure. In particular, using the MINITAB software, the distributions of all steps were calculated, verifying how the experimental data are well interpolated by a normal distribution. The sensitivity of the fiber alone to pressure variation amounts to 3.04e-3 nm/MPa; so the development of a geometry capable of amplifying the pressure effect is essential. Different architectures for pressure transducer development have already validated the possibility of varying the sensitivity values. Higher sensitivities have been achieved using sensors positioned perpendicular to the membrane itself. In the case of these geometries, it has been possible to achieve significant sensitivities ranging from 7 nm/MPa to 31.67 nm/MPa. For geometries where the sensor is instead placed parallel to the transducer membrane, sensitivities range from 8e-2 nm/MPa to 5.28 nm/MPa [31-38].

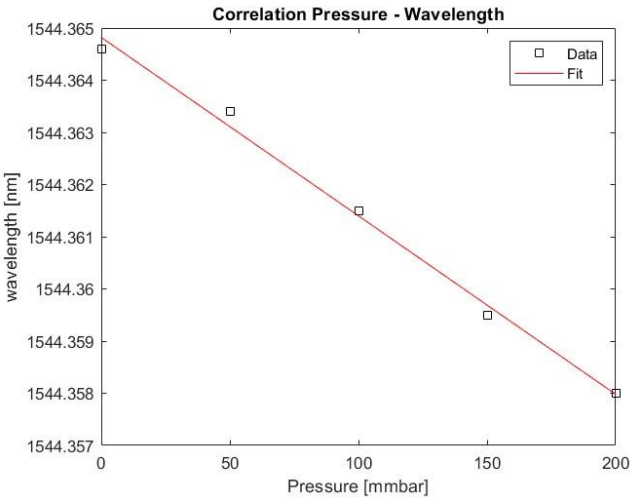

Figure 11 Sensor calibration curve.

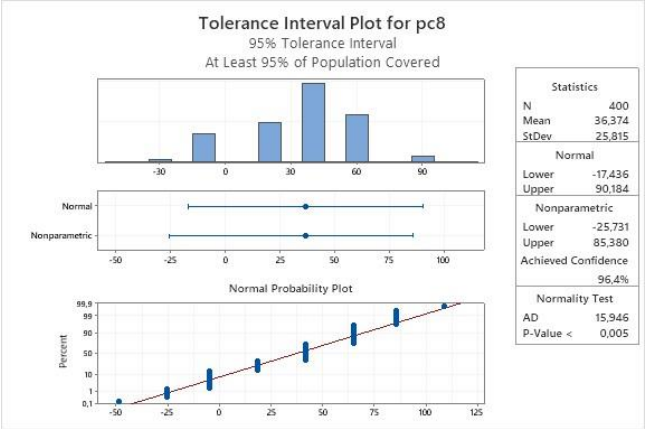

Figure 12 Overall statistic step validation.

6 CONCLUSIONS

In this paper, the design, sensitivity methodology, fabrication and experimental validation of a pressure sensor using FBG sensors was described. At first, the designed geometry allowed the realization of an extremely simple and customizable mould. Moreover, it was designed to be fabricated by additive manufacturing, thus ensuring reliability, repeatability but also low cost. The experimental campaign demonstrated the functionality of the proposed proof of concept and a sensitivity comparable to the amplitude of the measurement steps taken, i.e., estimated to be 50 mbar. Statistical analysis demonstrated excellent reliability of the measured wavelength data. There is evidence of great repeatability of the data obtained at the same pressure imposed by the system, as well as a normal distribution of the experimental data over each of the experimental steps. Moreover, a linear correlation between pressure and wavelength was find, so allowing to validate the statistical data distribution also for data converted in pressure. Thanks to the great results achieved in this work, authors are encouraged to continue the research by focusing on other specific materials that could be employed to maximize performances and pressure range applicability.

REFERENCES

[1] L. Borello, G. Villero and M. D. L. Dalla Vedova, Flap failure and aircraft controllability: Developments in asymmetry monitoring techniques. *Journal of Mechanical Science and Technology*, 2014.

[2] D. Belmonte, M. D. L. Dalla Vedova and P. Maggiore, Prognostics of onboard electromechanical actuators: A new approach based on spectral analysis techniques. *International Review of Aerospace Engineering*, Vol. 11, No. 3, pp. 96-103, 2018.

[3] Safa. Kasap, *Optoelectronics and photonics : principles and practices*. Prentice Hall, 2001.

[4] C. Hong, Q. Yang, X. Sun, W. Chen and K. Han, A theoretical strain transfer model between optical fiber sensors and monitored substrates. *Geotextiles and Geomembranes*, Vol. 49, No. 6, pp. 1539-1549, 2021.

[5] M. J. Matthewson, *Optical fiber mechanical testing techniques*. Vol. 10272, pp. 34-61, 1993.

[6] A. Aimasso, G. Charruaz, M. Bertone, C. Ferro, M. D. L. Dalla Vedova and P. Maggiore, Test bench and control logic development for dynamic thermal characterization of optical sensors. *International Journal of Mechanics and Control*, Vol. 24, No. 2, pp. 69-76, 2023.

[7] X. Qiao and Q. Rong, FBG for Oil and Gas Exploration. *Journal of Lightwave Technology*, Vol. 37, No. 11, pp. 2502-2515, 2019.

[8] P. Rajeev, J. Kodikara, W. K. Chiu and T. Kuen, Distributed Optical Fibre Sensors and their Applications in Pipeline Monitoring. *Key Eng Mater*, Vol. 558, pp. 424-434, 2013.

[9] U. Utzinger and R. R. Richards-Kortum, Fiber optic probes for biomedical optical spectroscopy. *J Biomed Opt*, Vol. 8, No. 1, p. 121, 2003.

[10] J. A. C. Heijmans, L. K. Cheng and F. P. Wieringa, Optical fiber sensors for medical applications - Practical engineering considerations. *IFMBE Proc*, Vol. 22, pp. 2330-2334, 2008.

[11] C. K. Y. Leung et al., *Review: optical fiber sensors for civil engineering applications*.

[12] A. A. Suryandi, N. Sarma, A. Mohammed, V. Peesapati and S. Djurović, Fiber Optic Fiber Bragg Grating Sensing for Monitoring and Testing of Electric Machinery: Current State of the Art and Outlook. *Machines*, Vol. 10, No. 11, p. 1103, 2022.

[13] A. Rovera, A. Tancau, N. Boetti, M. D. L. Dalla Vedova, P. Maggiore and D. Janner, Fiber Optic Sensors for Harsh and High Radiation Environments in Aerospace Application. *Sensors* 2023, Vol. 23, No. 5, p. 2512, 2023.

[14] E. J. Friebele et al., Optical fiber sensors for spacecraft applications. *Smart Mater. Struct*, Vol. 8, pp. 813-838, 1999.

[15] A. Behbahani, M. Pakmehr and W. A. Stange, Optical Communications and Sensing for Avionics. *Springer Science and Business Media Deutschland GmbH*, 2020.

[16] C. Lopatin, Aerospace Applications of Optical Fiber Mechanical Sensors. *Opto-Mechanical Fiber Optic Sensors: Research, Technology, and Applications in Mechanical Sensing*, Elsevier Inc., pp. 237-262, 2018.

[17] A. Aimasso, Optical fiber sensor fusion for aerospace systems lifecycle management, in *Materials Research Proceedings*, 2023.

[18] S. J. Mihailov, Fiber Bragg Grating Sensors for Harsh Environments. *Sensors*, 2012.

[19] R. Rodríguez-Garrido et al., High-temperature monitoring in central receiver concentrating solar power plants with femtosecond-laser inscribed fbg. *Sensors*, 2021.

[20] G. P. Agrawal and S. Radic, Phase-Shifted Fiber Bragg Gratings and their Application for Wavelength Demultiplexing. *IEEE Photonics Technology Letters*, 1994.

[21] S. J. Mihailov et al., *Extreme Environment Sensing Using Femtosecond Laser-Inscribed Fiber Bragg Gratings*.

[22] A. Aimasso, M. D. L. Dalla Vedova and P. Maggiore, Analysis of FBG Sensors Performances When Integrated Using Different Methods for Health and Structural Monitoring in Aerospace Applications. *6th International Conference on System Reliability and Safety*, ICSRS 2022, 2022.

[23] A. Aimasso and C. G. Ferro, Proposal of a Standard Method to Define a Best Practice for Bonding FBG Sensors for Aerospace Use. in 2023 IEEE *10th International Workshop on Metrology for AeroSpace, MetroAeroSpace 2023* - Proceedings, 2023.

[24] A. Aimasso, G. Gallone, M. D. L. Dalla Vedova, and P. Maggiore, Experimental analysis of FBG sensors thermal calibration under different loading conditions. *2023 IEEE 10th International Workshop on Metrology for AeroSpace, MetroAeroSpace 2023 - Proceedings*, pp. 621-626, 2023.

[25] A. Aimasso, M. D. L. Dalla Vedova, D. Janner, P. Maggiore and A. Rovera, Influence of adhesive and application method on FBG temperature sensors for space applications. *2023 IEEE 10th International Workshop on Metrology for AeroSpace, MetroAeroSpace 2023 - Proceedings*, pp. 492-497, 2023.

[26] A. Aimasso, C. G. Ferro, M. Bertone, M. D. L. Dalla Vedova and P. Maggiore, Fiber Bragg Grating Sensor Networks Enhance the In Situ Real-Time Monitoring Capabilities of MLI Thermal Blankets for Space Applications. *Micromachines*, Vol. 14, No. 5, 2023.

[27] C. G. Ferro, A. Aimasso, M. Bertone, N. Sanzo, M. D. L. D. Vedova and P. Maggiore, Experimental development and evaluation of a fiber bragg grating-based outside air temperature sensor for aircraft applications. *Transportation Engineering*, Vol. 14, 2023.

[28] M. D. L. Dalla Vedova, P. C. Berri, and A. Aimasso, Environmental sensitivity of Fiber Bragg Grating sensors for aerospace prognostics. *Proceedings of the 31st European Safety and Reliability Conference, ESREL 2021*, 2021.

[29] A. C. Marceddu, A. Aimasso, S. Schiavello, B. Montrucchio, P. Maggiore and M. D. L. Dalla Vedova, Comprehensive Visualization of Data Generated by Fiber Bragg Grating Sensors. IEEE *Access*, Vol. 11, 2023.

[30] Marceddu A. C., Quattrocchi G., Aimasso A., Giusto E., Baldo L., Vakili M. G., Vedova M. D. L. D., Montrucchio B. and Maggiore P., Air-To-Ground Transmission and Near Real-Time Visualization of FBG Sensor Data Via Cloud Database. *IEEE Sensor Journal*, 2022.

[31] M. Fu Liang, X. Qiu Fang, G. Wu, G. Zhe Xue and H. Wei Li, A fiber bragg grating pressure sensor with temperature compensation based on diaphragm-cantilever structure. *Optik*, 2017.

[32] E. Vorathin, Z. M. Hafizi, N. Ismail and M. Loman, Review of high sensitivity fibre-optic pressure sensors for low pressure sensing. *Optics and Laser Technology*, Vol. 121, 2020.

[33] Y. Zhu and A. Wang, Miniature fiber-optic pressure sensor. *IEEE Photonics Technology Letters*, Vol. 17, No. 2, pp. 447-449, 2005

[34] P. V. Rao, K. Srimannarayana, M. S. Shankar, P. Kishore and S. R. Prasad, *Enhanced Sensitivity of FBG Pressure Sensor Using Thin Metal Diaphragm*.

[35] G. Allwood, G. Wild, A. Lubansky and S. Hinckley, A highly sensitive fiber Bragg grating diaphragm pressure transducer. *Optical Fiber Technology*, Vol. 25, pp. 25-32, 2015,

[36] A. Leal-Junior, A. Frizera and C. Marques, A fiber Bragg gratings pair embedded in a polyurethane diaphragm: Towards a temperature-insensitive pressure sensor. *Opt Laser Technol*, Vol. 131, 2020.

[37] X. Wang, B. Li, O. L. Russo, H. T. Roman, K. K. Chin and K. R. Farmer, Diaphragm design guidelines and an optical pressure sensor based on MEMS technique. *Microelectronics J*, Vol. 37, No. 1, pp. 50-56, 2006.

[38] V. Rao Pachava, S. Kamineni, S. Shankar Madhuvarasu and K. Putha, A high sensitive FBG pressure sensor using thin metal diaphragm. *Journal of Optics*, Vol. 43, No. 2, pp. 117-121, 2014.